Clays and Clay Minerals, Vol. 31, No. 4, 241–250, 1983.

THERMAL TRANSFORMATION OF ANTIGORITE AS STUDIED BY ELECTRON-OPTICAL METHODS

HELENA DE SOUZA SANTOS AND KEIJI YADA

Laboratório de Microscopia Eletrônica, Instituto de Física
Universidade de São Paulo, São Paulo, Brasil and
Research Institute for Scientific Measurements, Tohoku University, Sendai, Japan

Abstract—The thermal transformation of a Brazilian antigorite heated dry from 600° to 1300°C, was studied by high resolution electron microscopy and selected area electron diffraction (SAD). Below 600°C, the antigorite particles did not change morphologically or crystallographically, as evidence by the presence of the superlattice in the SAD patterns and lattice images. At 650°C, traces of antigorite remained, although the superlattice structure had disappeared and the first indications of forsterite formation were observed in the same SAD. Diffraction patterns of the transition phases showed various topotactical relationships between antigorite and forsterite. At 800°C, the crystallization to forsterite was much more pronounced. At 900°C, the individual particles retained their original shapes, but they were actually pseudomorphs, for their SAD patterns showed only forsterite. Between 1000° and 1300°C various topotactical relationships were observed. Although the overall transformation to forsterite appears to be similar for both chrysotile and antigorite, the transformation of antigorite took place at a slightly higher temperature (~50°C) with a larger number of topotactical relationships than for chrysotile. Enstatite was formed at 1300°C, but it was impossible to determine the topotactic relations between enstatite and forsterite, which was possible with chrysotile.

Key Words—Antigorite, Asbestos, Chrysotile, Forsterite, Lattice image, Selected area electron diffraction, Serpentine, Topotactic structure.

INTRODUCTION

The thermal dehydration and subsequent recrystallization of both platy and fibrous serpentine minerals has been the subject of many investigations (e.g., Brindley and Zussman, 1957). The principal recrystallization product, forsterite, forms topotactically, i.e., with well-defined crystallographic orientations with respect to the parent crystal structure. The thermal transformation of chrysotile, heated dry from 600° to 1300°C, was studied using high resolution electron microscopy and selected area electron diffraction (SAD) by Souza Santos and Yada (1979). They showed that forsterite formed in at least two orientations: the fiber direction or *a* of the chrysotile became *b* direction of forsterite; the other orientations are derived from the first by rotations of ±60° about *a* direction of forsterite. They emphasized that the angular values of the orientation relationships established by X-ray diffraction analysis when measured by electron-optical methods presented differences up to several degrees.

In a continuation of the earlier study of chrysotile, a thermal investigation of the serpentine mineral antigorite was carried out to determine the effect of the morphological differences between platy antigorite and cylindrical chrysotile on the orientation of the forsterite formed, and also to examine the behavior of the antigorite superlattice after heat treatments.

MATERIALS AND METHODS

For this study, the specimen used was a very white clay from Castro, Paraná, Brazil, studied by Brindley and Souza Santos (1971). It is essentially pure antigorite occurring as a clay-size material. Its chemical analysis showed 0.33% Al_2O_3 and 0.41% Fe_2O_3, very low values for these oxides compared with other antigorite (Brindley and Zussman, 1957).

To observe the effect of the thermal treatment by electron microscopy, two methods of sample preparation were employed. In the first method, the antigorite was finely ground in an agate mortar and sample heated in an electric furnace for 8-hr periods at successively higher temperatures, from 600° to 1300°C. After heating at the desired temperatures, the samples were left to cool overnight. Samples heated in this manner were prepared by the suspension method for transmission electron microscopy: a small droplet of antigorite particles suspended in distilled water was dried in air on a microgrid (perforated film) reinforced with evaporated carbon. The particles spanning the holes, without a supporting film underneath, were subjected to observation and photographic registration. In the second method, duplicate samples were mounted on microgrids and observed electronmicroscopically and then were heated in a micro-electrical furnace. This furnace consists of an alumina tube with an externally wrapped nickel-chromium electric heater covered concentrically by a larger alumina tube and a still larger stainless steel tube for heat shielding. The equipment was submitted to a high vacuum, and the micro-furnace was heated to the desired temperature for 20–30 min by an alternate current controlled by a Variac transformer. The temperature, up to 900°C, was monitored by a plat-

inum/platinum-rhodium thermocouple attached to a galvanometer. This second method produced a different heating environment and heating time from the first method, and is thought to have the advantage of assuring that the morphological and crystallographic changes are really due to the heat treatment. Heating in vacuum provided a controlled neutral atmosphere; in contrast to the first method, no differences were observed which could be attributed to ferrous iron oxidation and/or to the low R_2O_3 content (Brindley and Souza Santos, 1971). The micro-furnace method also allowed the effects of progressively higher temperatures to be followed in the same area of the same grid, whereas in the first method, different particles were observed in different grids.

A Siemens Elmiskop 101 transmission electron microscope with a pointed filament was used at 100 kV. The microscope was modified to reduce both spherical and chromatic aberrations by employing the "pole-piece-in-polepiece" system (Yada and Kawakatsu, 1976), and by increasing the excitation of the objective lens. The direct electron-optical magnification employed was 40,000× to 300,000×. The selected area electron diffraction (SAD) method was used exclusively, and the orientation of the crystalline image with respect to its SAD pattern was estimated from a rotation calibration curve.

RESULTS

The antigorite sample consists of individual particles (about 0.5 to 2 μm in size) that exhibit a variable morphology in the transmission electron microscope (Brindley and Souza Santos, 1971); many have thin rectangular platy forms, some are rod-shaped, and others present a peculiar morphology with holes through them. The platy crystals are oriented with the basal (001) planes parallel to the plane of the stage of the instrument, and single-crystal diffraction patterns show the (hk0) diffraction typical of antigorite, with closely spaced clusters of spots running along the a^* direction, corresponding to the values of a (Brindley and Souza Santos, 1971). The superlattice parameter a varies from 38.5 to 47.8 Å from one crystal to another. The 020 reflections, corresponding to 4.6-Å spacing, was used as an intermediate standard for these measurements. In the rod-shaped crystals, the elongation appears to be parallel to the b-axis of antigorite, when observed with the (001) basal plane normal to the stage. If a specimen lying on (001) plane is tilted around the a-axis, the 020 reflections of the electron diffraction pattern are split, as seen in Figure 1A. The (020) fringes, corresponding to a spacing of 4.6 Å, from such specimens have a wavy appearance as shown in Figure 1B, which can be considered as a characteristic reflection of the corrugated structure of antigorite (Yada, 1979).

The differential thermal analysis curve of the Castro antigorite contains a broad endothermic reaction starting at about 600°C, with a peak at about 760°C, caused by dehydroxylation of the mineral, and a sharp exothermic peak at about 830°C, caused by the formation of forsterite (Brindley and Souza Santos, 1971). The heat treatment from 600° to 1300°C caused very little change in the appearance of the crystals or in their physical properties. The original very white color was maintained throughout the temperature range studied. Also the crystals retained their soft quality and still crumbled easily and dispersed readily in water, but proved to be difficult to shear into sufficiently thin particles for high resolution electron microscopy; thus the investigation was more difficult than the earlier chrysotile study (Souza Santos and Yada, 1979). Throughout the tem-

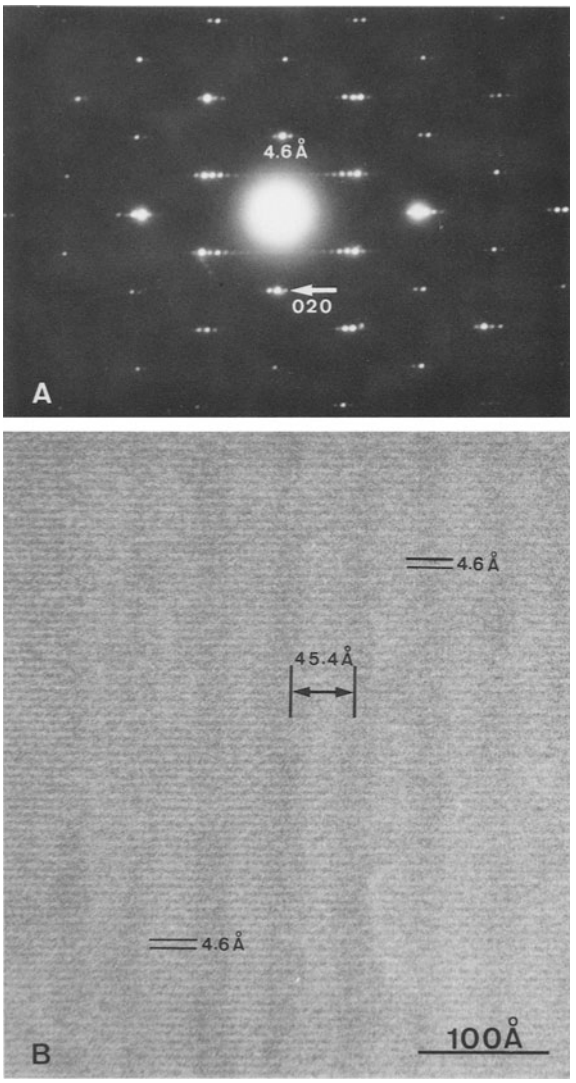

Figure 1. (A) Selected area diffraction (SAD) pattern of antigorite, tilted around the a-axis. (B) The lattice image of a tilted specimen showing a wavy structure perpendicular to the b-axis. The 4.6-Å spacing and the 45.4-Å a parameter are indicated.

https://doi.org/10.1346/CCMN.1983.0310401 Published online by Cambridge University Press

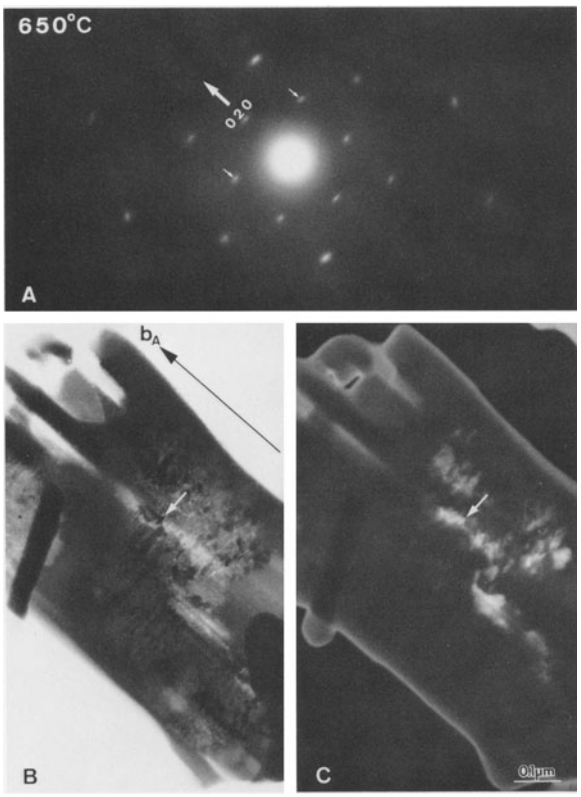

Figure 2. (A) SAD pattern of antigorite heated to 650°C. The diffraction spots are faint and are not split into characteristic superlattice groups. (B) Micrograph shows the beginning of forsterite formation, as mosaic structures. (C) Dark field images confirm the crystallinity of such grains (arrows).

perature range studied, SAD patterns were taken to identify the phases present, and to determine what preferred orientations each phase possessed.

<600°C

Below 600°C the antigorite particles did not change morphologically or crystallographically; superlattice effects were always recorded in the SAD patterns and in the high resolution images.

650°C

At 650°C only traces of antigorite and the first indication of forsterite formation was found in the same crystal. Both patterns were observed in the same SAD pattern, so it was possible to establish the orientation between the two minerals. Moreover, both in the lattice image and in the SAD patterns, the antigorite superlattice structure had disappeared. In the SAD patterns, the spots were faint, diffuse, and not split into characteristic superlattice groups or clusters (Figure 2A). Micrographs showed the beginning of forsterite formation, as mosaic structures, consisting of fine subgrains inside the original particles of antigorite (Figure 2B). The crystallinity of such grains was clearly demonstrated by dark field images (Figure 2C).

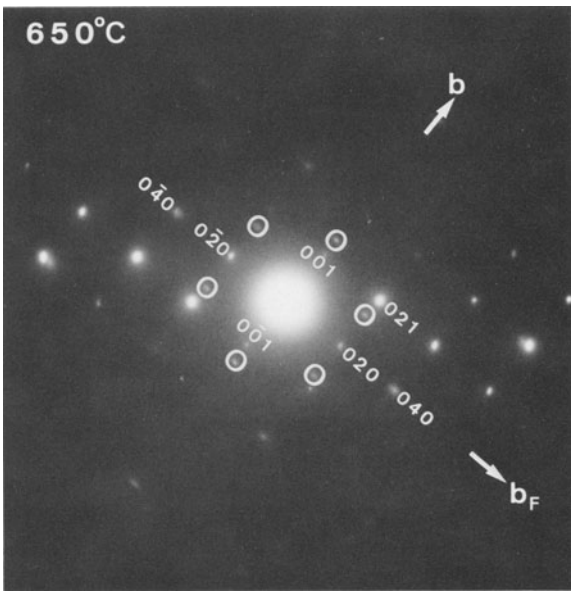

Figure 3. SAD pattern (650°C) shows various topotactical relations between antigorite (circles) and forsterite (index).

The SAD patterns of this transition phase showed various topotactical relations between antigorite and the newly formed forsterite. Most relationships were similar to those previously observed in chrysotile (Souza Santos and Yada, 1979), but some new relationships were observed. In Figure 3 the orientation of forsterite with respect to the original antigorite $a_A \parallel b_F$, $b_A \parallel c_F$, and $c_A \parallel a_F$ is shown, where the subscripts F and A refer respectively to forsterite and antigorite. The a–b plane of antigorite parallel to the b–c plane of forsterite was the most common relationship observed. This was also the case for chrysotile (Souza Santos and Yada, 1979).

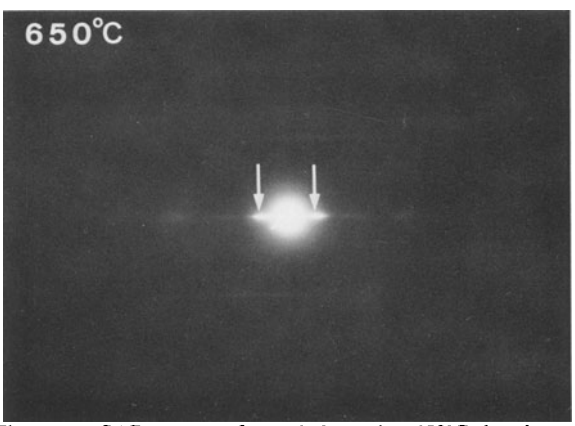

Figure 4. SAD pattern of sample heated to 650°C showing a new reflection corresponding to a 12–13-Å spacing (arrows).

https://doi.org/10.1346/CCMN.1983.0310401 Published online by Cambridge University Press

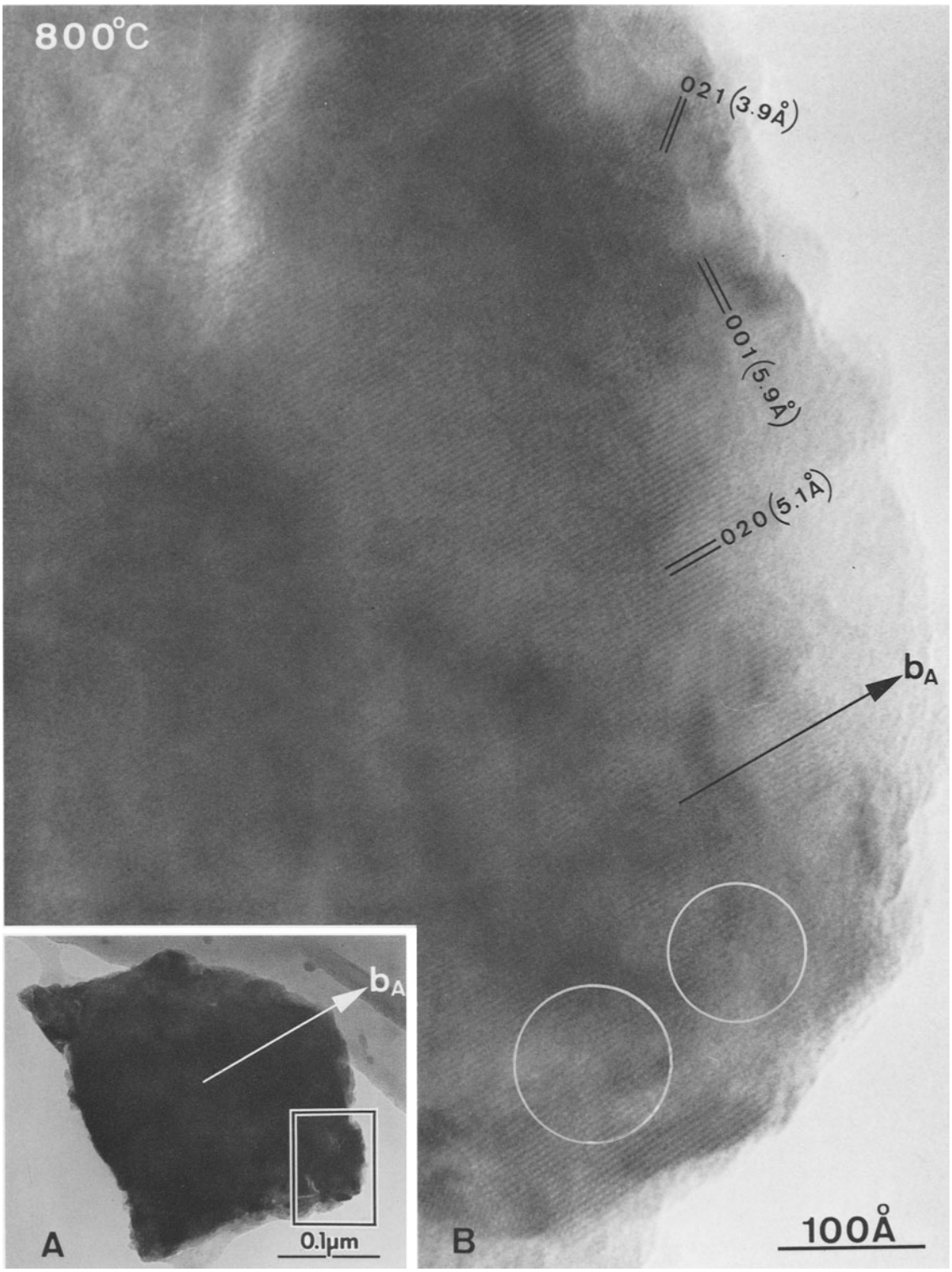

Figure 5. (B) Lattice image (800°C) of indicated area in (A), showing three fringe systems of 3.9 Å, 5.1 Å, and 5.9 Å (2 × 2.99 Å) corresponding respectively to the (021), (020), and (001) planes of forsterite. The 5.1-Å fringe system, which is in the forsterite *c*-axis direction, is parallel to antigorite *b*-axis. Dislocations are indicated by circles.

https://doi.org/10.1346/CCMN.1983.0310401 Published online by Cambridge University Press

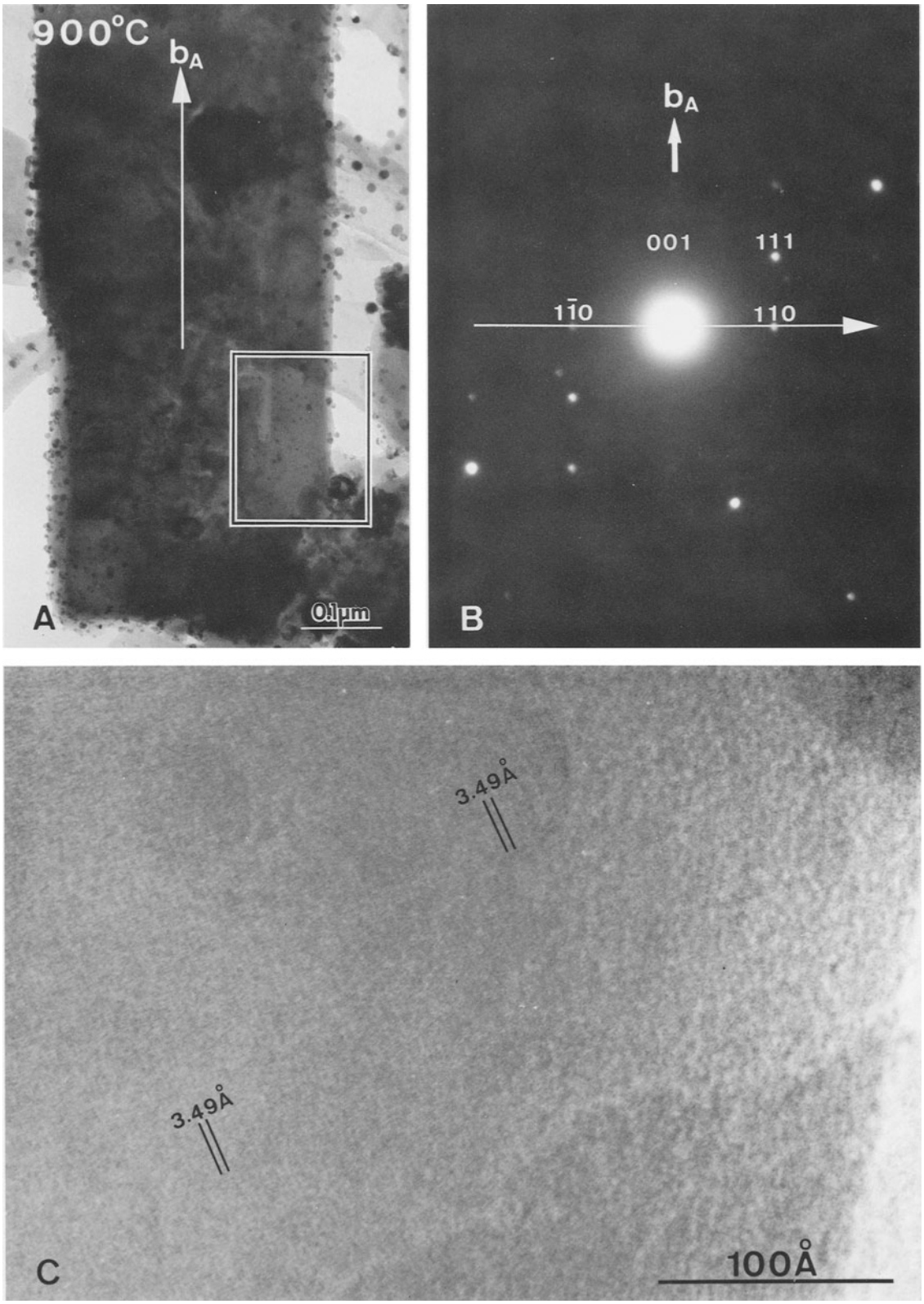

Figure 6. Morphology (A) and SAD pattern (B) from sample heated to 900°C, showing a new relation: $a_A \parallel \langle 110 \rangle_F$. (C) The corresponding lattice image (indicated area in A), presents the fringe system of a 3.49-Å spacing corresponding to (111) plane of forsterite.

https://doi.org/10.1346/CCMN.1983.0310401 Published online by Cambridge University Press

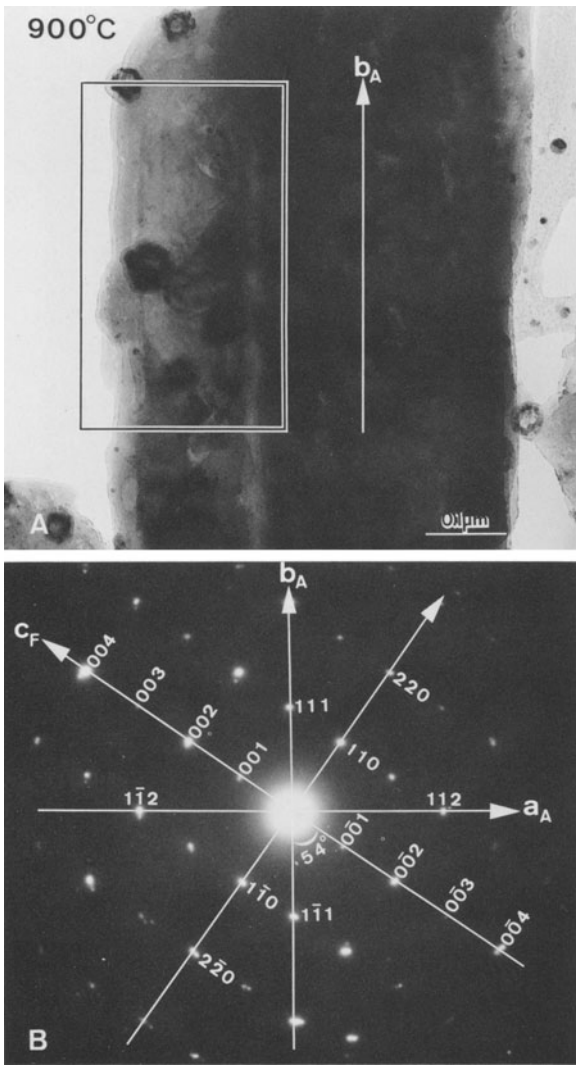

Figure 7. Morphology (A) and SAD pattern (B) from sample heated to 900°C, showing a new topotactic relation: $b_A \parallel \langle 111 \rangle_F$ making a 54° angle with c_F axis, and $a_A \parallel \langle 11\bar{2} \rangle_F$.

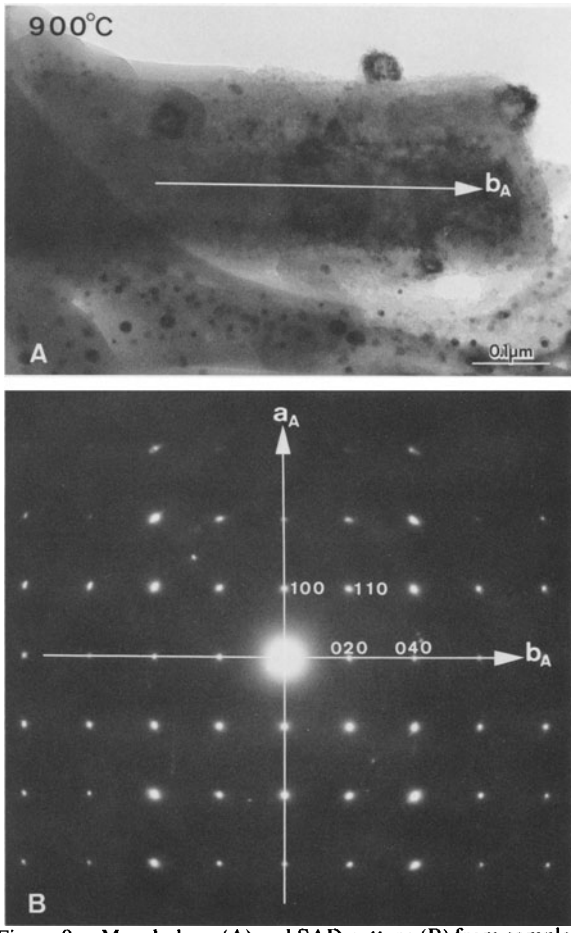

Figure 8. Morphology (A) and SAD pattern (B) from sample heated to 900°C, present another relation: $a_A \parallel a_F$; $b_A \parallel b_F$; $c_A \parallel c_F$ (1000°C).

Some SAD pattern showed a broad reflection corresponding to a long spacing of about 12 to 13 Å in the *c*-direction of antigorite (Figure 4).

700°C

At 700°C antigorite and forsterite were both still present, but now enhanced forsterite patterns were present in the SAD patterns.

800°C

At 800°C the crystallization to forsterite had taken place to a much more advanced stage. The individual particles still had the original antigorite morphology but were pseudomorphs made up of forsterite, easily identified by the SAD patterns.

Many micrographs showed fringe systems of forsterite. Figure 5B, a high resolution electron micrograph of Figure 5A, is an example of the lattice image showing three fringe systems, 3.9 Å, 5.1 Å, and 5.9 Å (2 × 2.99 Å), corresponding to the (021), (020), and (001) planes of forsterite, respectively. The 5.1 Å fringe system, in the direction of the *c*-axis of forsterite, can be observed parallel to the *b*-axis of antigorite. From this lattice image, it can again be observed that $a_A \parallel b_F$ and $b_A \parallel c_F$. These fringe systems were not always uniform but, as indicated by circles in Figure 5B, extra half planes of dislocations occurred suggesting that the nucleation sites of forsterite in antigorite were fairly abundant, as suggested by Figures 2A and B.

900°C

At 900°C many of the individual particles kept the original shape of the antigorite but had completely transformed to forsterite as shown by the morphology and SAD pattern in Figures 6A and B. The dark specks in Figure 6A are not nuclei, but noncrystalline material

https://doi.org/10.1346/CCMN.1983.0310401 Published online by Cambridge University Press

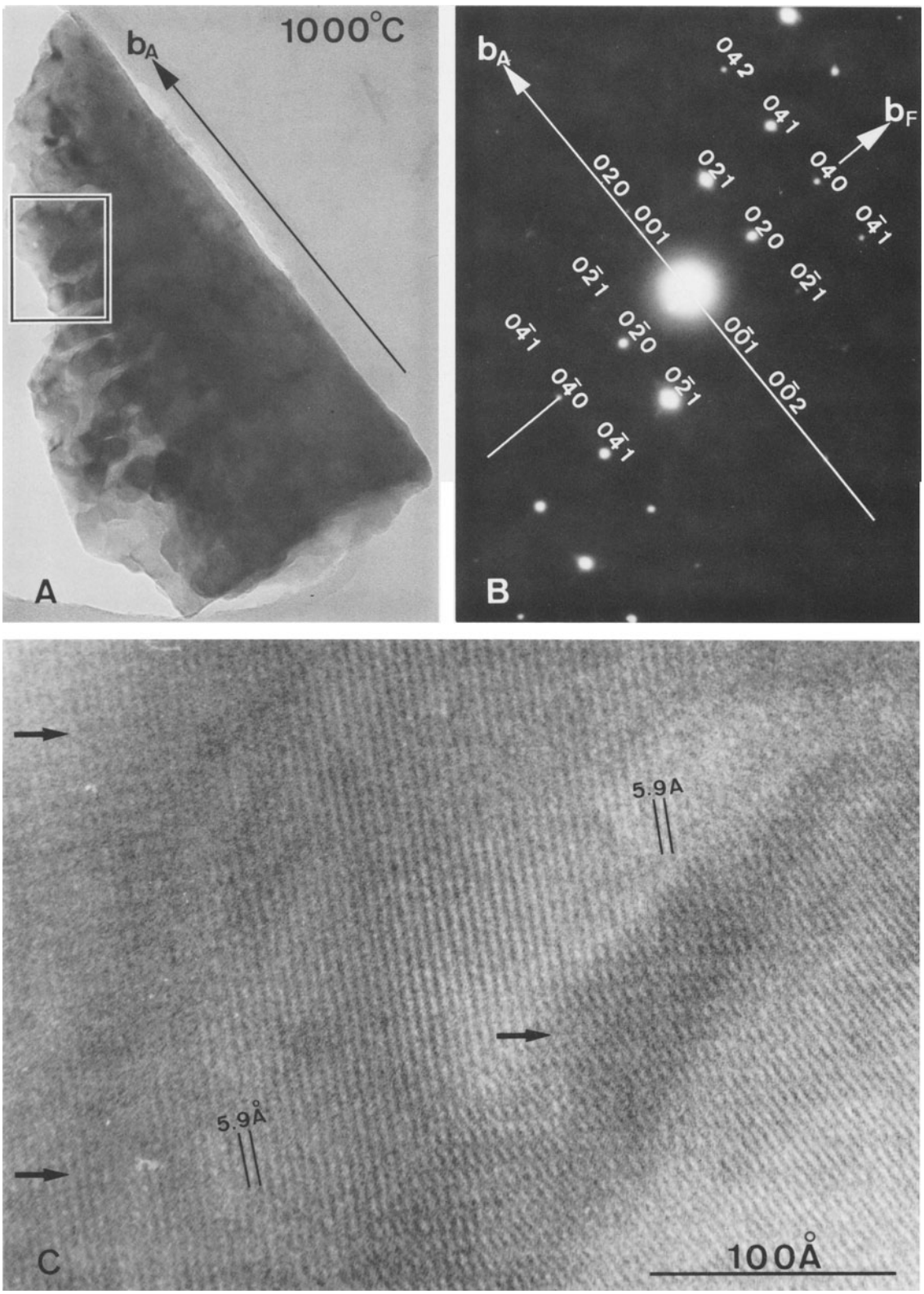

Figure 9. From morphology (A) and SAD pattern (B) from sample heated to 1000°C, the following relationships can be seen: $b_A \parallel c_F$ and $a_A \parallel b_F$. The lattice image shows, from the indicated area in (A), the fringe system of a 5.9-Å spacing. Moiré fringes (arrows) suggest that forsterite is not a perfect single crystal.

https://doi.org/10.1346/CCMN.1983.0310401 Published online by Cambridge University Press

from the micro-furnace used during the heat treatment. In this figure a new relation can be observed: $a_A \parallel \langle 110 \rangle_F$ and $b_A \parallel c_F$.

The corresponding lattice image (Figure 6C), which is a high resolution image of Figure 6A, presents the 3.49 Å fringe system which corresponds to the (111) plane of forsterite.

Another topotactic relation can be seen from the SAD pattern and morphology in Figures 7A and B. The SAD pattern of forsterite is similar to Figure 6B but the directions of a_A and b_A are quite different from previous relationships and $b_A \parallel \langle 111 \rangle_F$, making an 54° angle with the *c*-axis, and $a_A \parallel \langle 11\bar{2} \rangle_F$. Another relationship is displayed in Figures 8A and B, where forsterite is in a (001) orientation and the orientations $a_A \parallel a_F$, $b_A \parallel b_F$, and $c_A \parallel c_F$ can be deduced.

1000°C

Only forsterite is present at 1000°C. From Figures 9A and B—morphology and SAD pattern—the following relationships can be drawn: $b_A \parallel c_F$ and $a_A \parallel b_F$. The lattice image shows the fringe system of the 5.9-Å spacing (Figure 9C). Moiré fringe, indicated by arrows, suggest that the forsterite is not a perfect single crystal but has slightly misoriented thin layers grown from individual nucleation sites.

1300°C

The transition to enstatite was observed at 1300°C; however, it was impossible to observe in the electron microscope the topotactic relations of enstatite to forsterite as was the case with chrysotile (Souza Santos and Yada, 1979).

DISCUSSION AND CONCLUSIONS

The broad reflection on and along the zero line, corresponding to a 12–13-Å spacing developed in antigorite at 650°C, corresponds to the intermediate metastable phase that was frequently observed at 600°C in chrysotile (Souza Santos and Yada, 1979). It was more difficult to observe in the present study because the antigorite crystals were oriented with the basal (001) cleavage planes parallel to the film-support. Thus, only when a crystal was favorably oriented by chance was this broad reflection observed. The position of this peak varies for different serpentine minerals (Brindley and Zussman, 1957) from about 14–15 Å as observed in chrysotile (Souza Santos and Yada, 1979) to 12–13 Å for some antigorites. The nature of such a peak in the thermal transformation of serpentine minerals has been discussed previously (Brindley and Wan, 1975, 1978). According to Brindley (1980), the close crystal-chemical relations between serpentine minerals, more particularly aluminous serpentine, and chlorites suggest that a partial transformation occurs towards a chlorite-like phase.

Brindley and Zussman (1957) reported that about 575°–600°C forsterite peaks are observed followed by complete disappearance of the serpentine pattern. In the present study, both antigorite and forsterite could be detected in the same crystal at 650°C, probably due to the smaller size of the crystals. Thus, recrystallization followed very shortly after dehydroxylation, which started at 600°C, in contrast to chrysotile, where forsterite only started to form above 700°C (Souza Santos and Yada, 1979).

At 650°C dehydroxylation occurred and the antigorite superlattice disappeared, as is quite evident in the SAD patterns and lattice images. Brindley and Zussman (1957) pointed out that considerable reorganization of the serpentine layers takes place when dehydroxylation occurs, accompanied by a collapse of the layer structure which will eventually recrystallize into forsterite. The antigorite superlattice has been attributed to the curvature of the serpentine layer about its *b*-axis in such a way as to form a corrugation parallel to *b*, the periodicity of these corrugations being *a* (Brindley *et al.*, 1958; Deer *et al.*, 1966). It is possible that the transformation into forsterite is preceded by a flattening of the curved antigorite layers, due to dehydroxylation effects. According to Brindley (1963) there must be a contraction of about 4% to form forsterite; in other words, 8 unit cells of serpentine develop, in an orderly way, into 9 unit cells of forsterite.

Starting at 650°C, the newly formed forsterite showed several different orientations with respect to the original antigorite crystals, as follows:

(A)	$a_A \parallel b_F$,	$b_A \parallel c_F$,	and	$c_A \parallel a_F$
(B)	$b_A \parallel c_F$	and		$a_A \parallel \langle 110 \rangle_F$
(C)	$b_A \parallel \langle 111 \rangle_F$	and		$a_A \parallel \langle 11\bar{2} \rangle_F$
(D)	$a_A \parallel a_F$,	$b_A \parallel b_F$,	and	$c_A \parallel c_F$

Orientation (A) was most frequently encountered and the others are rather rare, though it is not clear if their occurrence is dependent on the temperature of heating. Thus, the new crystals of forsterite showed many more orientations with respect to the original antigorite crystals, than what was observed in chrysotile (Souza Santos and Yada, 1979).

Most of topotactic relationships in antigorite are probably related to crystalline and morphological differences between chrysotile and antigorite particles. Our observations (Figures 2A, 2B, 5B) show that the nucleation sites of forsterite inside the antigorite crystals are numerous and slightly misoriented; this is probably a consequence of the many defective regions which develop later into misoriented nuclei, due to the flattening of the corrugated layer, following dehydroxylation. As was pointed out above, the Moiré fringes shown in Figure 9C suggest that forsterite is not a perfect single crystal, but that it is actually composed of slightly misoriented thin layers grown from individual nucleation sites. Probably these layers, accommodated inside the

forsterite crystals in different orientations, favor the development of a great number of topotactical relationships. In tubular crystals of chrysotile, which do not flatten after dehydroxylation, only the relation: $a_A \parallel b_F$, $b_A \parallel c_F$, and $c_A \parallel a_F$ can develop due to the limitations in size and material imposed by the small diameter of the fibrils. A similar restriction to the growth of mullite needles in small volumes was observed in tubular kaolin mineral from Piedade (Campos *et al.*, 1976) when compared with their wide developments in platy kaolinite (Comer, 1960).

Although the final transformation (serpentine to forsterite) is closely similar for chrysotile and antigorite, the transformation from antigorite takes place at slightly higher temperature (by about 50°C) with richer topotactical relationships, than from chrysotile. Enstatite was formed at 1300°C, but it was not possible to determine the topotactic relations of enstatite to forsterite. This probably is due to the fact that the sample heated at 1300°C no longer cleaved so favorably, and the premounted sample was not heat treated to 1300°C.

ACKNOWLEDGMENTS

This work was supported by a grant from the "Conselho Nacional de Desenvolvimento Científico e Tecnológico" (CNPq TC 401122/79) to have Prof. Keiji Yada as Visiting Professor at the University of São Paulo. Part of this paper was presented at the 7th International Clay Conference held in Bologna, Italy, September 1981.

REFERENCES

Brindley, G. W. (1963) Role of crystal structure in solid state reactions of clays and related minerals: in *Proc. Int. Clay Conf., Stockholm, 1963, Vol. 1,* Th. Rosenqvist and P. Graff-Petersen, eds., Pergamon Press, Oxford, 37–44.

Brindley, G. W. (1980) Varieties of order and disorder in layer silicates: *Bull. Mineral.* **103,** 395–403.

Brindley, G. W., Comer, J. J., Uyeda, R., and Zussman, J. (1958) Electron optical observations with crystals of antigorite: *Acta Crystallog.* **11,** 99–102.

Brindley, G. W. and Souza Santos, P. (1971) Antigorite—its occurrence as a clay mineral: *Clays & Clay Minerals* **19,** 187–191.

Brindley, G. W. and Wan, H. M. (1975) Compositions, structures and thermal behavior of nickel-containing minerals in the lizardite-nepouite series: *Amer. Mineral.* **60,** 863–871.

Brindley, G. W. and Wan, H. M. (1978) The 14 Å phase developed in heated dickites: *Clay Miner.* **13,** 17–24.

Brindley, G. W. and Zussman, J. (1957) A structural study of the thermal transformation of serpentine minerals to forsterite: *Amer. Mineral.* **42,** 461–474.

Campos, T. W., Souza Santos, H., and Souza Santos, P. (1976) Mullite development from fibrous kaolin mineral: *J. Amer. Ceram. Soc.* **59,** 357–360.

Comer, J. J. (1960) Electron microscope studies of mullite development in fired kaolinites: *J. Amer. Ceram. Soc.* **43,** 378–384.

Deer, W. A., Howie, R. A., and Zussman, J. (1966) *An Introduction to the Rock-Forming Minerals:* Longmans, London, p. 244.

Souza Santos, H. and Yada, K. (1979) Thermal transformation of chrysotile studied by high resolution electron microscopy: *Clays & Clay Minerals* **27,** 161–174.

Yada, K. (1979) Microstructures of chrysotile and antigorite by high-resolution electron microscopy: *Can. Mineral.* **17,** 679–691.

Yada, K. and Kawakatsu, H. (1976) Magnetic objective lens with small bores: *J. Electronmicrosc. (Japan)* **25,** 1–9.

(Received 25 August 1982; accepted 4 January 1983)

Резюме—Термическая трансформация Бразилийского антигорита, нагретого в сухом состоянии от 600° до 1300°C, исследовалась при помощи сильно разрещающего электронного микроскопа и диффракции электронов на выбранных поверхностях (ДЭП). Ниже 600°C частицы антигорита не изменялись морфологически или кристаллографически, что было полтверждено присутствием супер-решетки в образцах ДЭП и образах решетки. При 650°C остались следы антигорита, хотя структура супер-решетки исчезла, и первые следы образования форстерита наблюдались в том же самом ДЭП. Образцы диффракции переходных фаз указывали на различные топотактические отношения между антигоритом и форстеритом. При 800°C кристаллизация форстерита была более видна. При 900°C индивидуальные частицы сохраняли начальную форму, но они были псевдоморфными, потому что их образцы ДЭП показали только форстерит. Различные топотактические отношения наблюдались между 1000° и 1300°C. Хотя трансформация в фостерит является полобной для обоих, антигорита и хризотила, трансформация антигорита происходила при немного большой температуре (~50°C) с большим числом топотактических отношений, чем для хризотила. Энстатит формировался при 1000°C, но определение топотактических отношений между энстатитом и форстеритом (как в случае хризотила) было невозможно. [E.G.]

Resümee—Die thermische Umwandlung von brasilianischem Antigorit, der trocken auf 600°–1300°C erhitzt wurde, wurde mittels hochauflösender Elektronenmikroskopie und Feinbereichselektronendiffraktion (SAD) untersucht. Unter 600°C veränderten sich die Antigoritteilchen weder morphologisch noch kristallographisch, wie durch die Anwesenheit von Überstrukturen in SAD-Diagrammen und in Gitterbildern bestätigt wird. Bei 650°C waren noch Spuren von Antigorit vorhanden, obwohl die Überstrukturen verschwunden waren, und die ersten Anzeichen einer Forsteritbildung im gleichen SAD-Diagramm beobachtet wurden. Die Diffraktionsdiagramme der Übergangsphasen zeigten verschiedene topotaktische Beziehungen zwischen Antigorit und Forsterit. Bei 800°C wurde die Kristallisation viel ausgeprägter. Bei 900°C hatten die einzelnen Teilchen noch ihre ursprüngliche Form, doch waren sie in Wirklichkeit Pseudomorphosen, da ihre SAD-Diagramme nur mehr Forsterit zeigten. Zwischen 1000° und 1300°C wurden verschiedene topotaktische Beziehungen beobachtet. Obwohl die endgültige Umwandlung in Forsterit für Chrysotil und Antigorit gleich zu sein scheint, findet die Umwandlung von Antigorit bei etwas höheren Temperaturen (um etwa 50°C) und mit einer größeren Zahl von topotaktischen Beziehungen statt als die von Chrysotil. Enstatit wurde bei 1300°C gebildet, aber es war unmöglich, die topotaktischen Beziehungen zwischen Enstatit und Forsterit zu bestimmen, wie es im Fall von Chrysotil möglich war. [U.W.]

Résumé—La transformation thermique d'une antigorite brésilienne chauffé au sec de 600°C à 1300°C a été étudiée par microscopie à électrons à resolution élevée et par diffraction d'électrons de region sélectionnée (SAD). Sous 600°C, les particules d'antigorite n'ont changé ni morphologiquement ni cristallographiquement, comme le met en evidence la présence du supertreillis des clichés SAD et des images de treillis. A 650°C, il restait des traces d'antigorite, quoique la structure du supertreillis avait disparu et les premières indications de la formation de forsterite avaient été observées dans le même SAD. Les clichés de diffraction des phases de transition ont montré des rapports topotactiques entre l'antigorite et la forsterite. A 800°C, la cristallisation en forsterite était beaucoup plus prononcée. A 900°C, les particules individuelles avaient gardé leurs formes d'origine, mais elles étaient en fait des pseudomorphes, car leur clichés SAD n'ont montré que de la forsterite. Entre 1000°C et 1300°C, des rapports topotactiques variés ont été observés. Quoique la transformation générale en forsterite semble être similaire pour la chrysotile et l'antigorite, la transformation en antigorite s'est produite à une température plus élevée (~50°C) avec une quantité plus élevée de rapports topotactiques que pour la chrysotile. De l'enstatite a été formée à 1300°C, mais il était impossible de determiner les rapports topotactiques entre l'enstatite et la forsterite, ce qui était possible avec la chrysotile. [D.J.]